ELSEVIER

Structure sensitive dissociation of CH$_4$ on Ni/α-Al$_2$O$_3$: Ni nano-scale particles linearly compensate the E_a and ln A for the CH$_4$ pulse kinetics

Yuehua Cui, Hengyong Xu *, Qingjie Ge, Yuzhong Wang, Shoufu Hou, Wenzhao Li

Dalian Institute of Chemical Physics, Chinese Academy of Sciences, P.O. Box 110, Dalian 116023, PR China

Abstract

The intrinsic kinetic information for the dissociation of CH$_4$ on the fresh Ni active sites was studied by pulsing CH$_4$ through Ni/α-Al$_2$O$_3$ catalyst with different Ni particles. After the elimination of the mass and heat transfer, the conversions of CH$_4$ were controlled far below the values of the thermodynamic equilibrium in order to keep the pulse reaction in the kinetic region. The coverage degree of carbon species on Ni active site is kept less than 1 to eliminate the influence of carbon deposition on the dissociation of CH$_4$. The plot of TOF$_{CH_4}$ versus the Ni particle size exhibits a "mountain" shape. The E_a and ln A for the CH$_4$ dissociation are linearly increased with the increase in the Ni particle size, showing the compensation effect in the CH$_4$ dissociation. This work reveals that the CH$_4$ dissociation on fresh Ni active site of Ni particles in Ni/α-Al$_2$O$_3$ catalysts is a structure sensitive reaction.
© 2006 Elsevier B.V. All rights reserved.

Keywords: CH$_4$ dissociation; Ni/α-Al$_2$O$_3$; Pulse kinetic; Structure sensitive; Compensation effect; Ni nano particle

1. Introduction

Methane as the major component of natural gas is being widely used for energy source and the production of fine chemicals. The synthesis gas obtained from the reforming reaction of CH$_4$ with CO$_2$ or H$_2$O can be further used to prepare oxygen-containing organic compounds [1] and highly pure hydrogen [2,3]. The carbon nanotubes and carbon fiber with special properties [4,5] can also be prepared by the dissociation of CH$_4$. Due to the cheapness, availability and high activity, Ni metal is considered as one excellent catalyst for CH$_4$ dissociation [1–5]. The study of CH$_4$ dissociation on Ni-based catalysts has received increasing interest due to its dual roles for science and application.

Liao and Zhang [6] calculated the activation energy (E_a) for CH$_4$ dissociation on metals Ru, Ir, Rh, Ni, Pd, Pt, Cu, Ag and Au and noted that Ni metal shows the lowest E_a. Other theoretical calculation, such as Hatree method [7], density function theory (DFT) [8] and ab initio [9] were used to calculate the E_a for the CH$_4$ dissociation on the different crystal plans of Ni metal. The

E_a of CH$_4$ dissociation on Ni(1 1 1), Ni(1 0 0) and Ni(1 1 0) has been obtained by experimental methods [10]. Recently, Egeberg et al. [11] obtained the E_a of CH$_4$ dissociation on Ni(1 1 1) as 74 ± 10 kJ/mol through the elimination of the carbon deposition. The present studies on the CH$_4$ dissociation mainly focus on one crystal plane of Ni metal [6–11], and most of the studies are theory calculation. However, the dissociation of CH$_4$ on the Ni-based catalysts is actually performed on various crystal planes of Ni particles, containing all the contribution of the various crystal plans of Ni particles.

Some experimental methods were also used to study the CH$_4$ dissociation on the Ni particles for the preparation of hydrogen or filamentous carbon [12–16]. This method involves the cumulative dissociation of CH$_4$ on Ni particles, in which the structure of Ni particles was also reported to change [15]. The carbon species coverage degree on the Ni active sites of catalysts becomes much higher than 1. CH$_4$ also dissociates on the Ni active sites which have deposited with the carbon species. The cumulative dissociation of CH$_4$ on Ni active sites does not disclose the intrinsic kinetic information for the single dissociation of CH$_4$ on the fresh Ni active sites of Ni particles.

In order to obtain the intrinsic kinetic information for the CH$_4$ dissociation on the fresh Ni active sites, the unsteady pulse method was used to investigate the dissociation of CH$_4$ on the

---

* Corresponding author. Tel.: +86 411 84581234; fax: +86 411 84581234.
  E-mail address: xuhy@dicp.ac.cn (H. Xu).

actual catalysts Ni/α-Al$_2$O$_3$, where the α-Al$_2$O$_3$ is a classical industrial support [17]. The pulse reaction greatly avoids the cumulative dissociation of CH$_4$ on Ni active sites and the coverage degree of carbon species on Ni sites was kept less than 1. And the pulse conversions of CH$_4$ dissociation were much lower than that of the thermodynamic equilibrium, which were controlled by kinetics. The pulse reaction directly gives the information of the intrinsic kinetic of CH$_4$ dissociation on the fresh Ni active sites of Ni particles in the Ni/α-Al$_2$O$_3$ catalysts. The experiment results show that the turn over frequency of CH$_4$ dissociation (TOF$_{CH_4}$) exhibits a "mountain" shape versus the Ni particle sizes in the pulse of CH$_4$ experiment. Herein, the Ni particles with different nano-scale have influence on the CH$_4$ dissociation. The obtained E_a and $\ln A$ of CH$_4$ dissociation have a good linear dependence on the particle size of Ni. The compensation effect between E_a and $\ln A$ for the CH$_4$ dissociation on Ni/α-Al$_2$O$_3$, results in the "mountain" shape of TOF$_{CH_4}$ versus Ni nano particle size. This work discloses that the dissociation of CH$_4$ on Ni particles of Ni/α-Al$_2$O$_3$ catalysts is a structure sensitive reaction and the E_a and $\ln A$ of CH$_4$ dissociation are linearly dependence on the Ni particle size.

2. Experimental

2.1. Catalysts and feed gases

All the catalysts were prepared by impregnating α-Al$_2$O$_3$ (2.1 m^2/g) with stoichiometric aqueous Ni(NO$_3$)·6H$_2$O for 12 h at room temperature (RT). The loading amount of Ni on the Ni/α-Al$_2$O$_3$ catalysts is 2, 4, 6 and 8 wt%. Then the catalysts were dried at 393 K for 3 h and calcined in air at 1073 K for 6 h. All the catalysts were in situ reduced by highly pure hydrogen at 1123 K for 0.5 h before used for the pulse reaction. CH$_4$ (99.995% purity), Ar (99.99% purity) and H$_2$ (99.99% purity) are used as feed gases.

2.2. X-ray diffraction (XRD) and H$_2$ chemisorption

XRD patterns were obtained with a Philips X′ Pert Highscore powder diffractometer (Cu Kα, 20° < 2θ < 80°). The particle sizes of Ni can be calculated based on Scherrer equation.

The exposed Ni atoms on Ni particles of Ni/α-Al$_2$O$_3$ were measured by H$_2$ chemisorption at RT by assuming H/Ni atomic ratio of 1. The samples of Ni/α-Al$_2$O$_3$ were reduced at 1123 K for 0.5 h then were decreased to 373 K under Ar and kept for 20 min, then further decreased to RT for in situ H$_2$ chemisorption measurement. The dispersion degree of Ni can be calculated as the ratio of N_0/Ni$_0$ × 100%, where N_0 is the exposed Ni atoms of per gram catalyst (atom/g cat) and Ni$_0$ is the total Ni atoms of per gram catalyst (atom/g cat).

2.3. Kinetic study

2.3.1. The elimination of inner and external diffusion

A quartz tube with dimension of 6 mm o.d. × 4 mm i.d. × 40 cm length was used as reactor. A thermocouple was introduced in the catalyst bed to measure the reaction tem-

perature. The Ar (50 ml/min) carries the CH$_4$ gas from quantitative tube (0.3058 ml) to the catalyst (5 mg) diluted by 50 mg quartz grain. The reactants and products were analyzed by an on-line GC (Model 103, TCD, carbon sieve as column).

The particle sizes of Ni/α-Al$_2$O$_3$ catalysts are 20–40, 40–60, 60–100, 100–160, 160–200 and 200–300 mesh and the according average grain diameters are 0.765, 0.54, 0.365, 0.175, 0.124 and 0.086 mm, respectively. The decrease in the particles size generally increases the CH$_4$ dissociation activity. When the activity does not increase with the decreasing of particle size any more, the inner diffusion can be eliminated.

The elimination of the external diffusion is carried out as follows. After the elimination of the inner diffusion, the particle size of catalysts is selected as 100–160 mesh. The flow rate of carrier gas is controlled in the range of 25–50 ml/min through the catalysts (2–10 mg). The carrier gas flow rate is changed to tune the contact time and finally make the activity of the reaction linearly dependence on the contact time. That means the external diffusion is eliminated.

2.3.2. CH$_4$ pulse reaction

A quartz tube with dimension of 6 mm o.d. × 4 mm i.d. × 40 cm length was used as the reactor. A thermocouple was introduced to the catalyst bed to measure the reaction temperature. The highly pure Ar (50 ml/min) was pulsed through the quantitative tube (0.3058 ml) to carry the CH$_4$ through the catalysts (5 mg) diluted with 50 mg quartz grain, which keeps the reforming reaction far away from the thermodynamic equilibrium. The reactants and products were analyzed by an on-line GC (Model 103, TCD, carbon sieve as column) and the conversions (shown in Tables 1 and 2) were calculated as follows:

$$\text{Con}_{\text{pul.}}\% = \frac{(\text{mol}_{\text{before pulse}} - \text{mol}_{\text{after pulse}})}{\text{mol}_{\text{before pulse}}} \times 100\% \qquad (1)$$

The coverage degree of carbon species on the catalyst can be calculated according to Eq. (2):

$$C_{\text{coverage}}(\%) = \frac{\text{Conv}_{\text{pul.}}\% V N_A}{22400(N_0 m)} \times 100\% \qquad (2)$$

Table 1
The parameters of the different Ni loading Ni/α-Al$_2$O$_3$ catalysts

Catalyst	Ni particle size[a] (nm)	The amount of active sites		Ni dispersion (%)[c]
		10^{19} sites/g cat[b]	10^{21} sites/g Ni[b]	
2%Ni	19.1	7.79	3.90	37.98
4%Ni	31.8	9.36	2.34	22.82
6%Ni	34.5	12.01	2.00	18.85
8%Ni	39.7	15.00	1.88	18.28

[a] Calculated from XRD results.
[b] Calculated by H$_2$-chemsorption by assuming H/Ni of 1.
[c] Calculated according to N_0/Ni$_0$, in which N_0 is the exposed Ni atoms of per gram catalyst (atom/g) and Ni$_0$ is the total Ni atoms of per gram catalyst (atom/g).

Table 2
The pulse results of CH_4 through the Ni/α-Al$_2$O$_3$ and the corresponding thermodynamic equilibrium value at different temperature

Catalyst	T (K)	Con (%)		Con$_{pul.}$/Con$_{equ.}$ (%)	$C_{coverage}$ (%)[c]	TOF[d] (s^{-1})
		Pul.[a]	Equ.[b]			
2%Ni	748	1.09	16.7	6.6	23.0	0.58
	773	1.63	32.3	5.0	34.4	0.86
	798	2.55	39.6	6.4	53.8	1.34
	823	3.04	45.8	6.6	64.1	1.60
4%Ni	748	1.74	16.7	10.4	30.6	0.76
	773	2.92	32.3	9.0	51.3	1.28
	798	3.49	39.6	8.8	61.3	1.65
	823	5.71	45.8	12.5	99.2	2.71
6%Ni	748	1.75	16.7	10.5	24.0	0.60
	773	2.92	32.3	9.0	40.0	1.00
	798	4.69	39.6	11.8	64.2	1.61
	823	5.92	45.8	12.9	81.1	2.03
8%Ni	748	1.68	16.7	10.1	18.4	0.45
	773	3.49	32.3	10.8	38.2	0.94
	798	4.47	39.6	11.3	49.0	1.20
	823	6.60	45.8	14.4	72.3	1.77

[a] Pulse experiment condition: Ar flow rate of 45–50 ml/min was pulse through the quantitative tube 0.3058 ml then through the catalysts 5 mg. The conversion of CH_4 was calculated to Eq. (1).
[b] Equilibrium conversion of CH_4 dissociation at the reaction condition calculated by the equilibrium constant.
[c] $C_{coverage}$ (%) was calculated base on Eq. (2).
[d] TOF was calculated base on Eq. (3).

TOF can be calculated according to Eq. (3):

$$TOF = \frac{Con_{pul.}\%(VN_A)}{22400t(N_0 m)} \qquad (3)$$

where V is the volume of quantitative tube (ml); N_A the Avogadro's constant (6.02×10^{23}/mol); N_0 the number of active sites per gram catalyst (sites/g cat); m the amount of catalyst (g); TOF the turn over frequency of CH_4 dissociation on one active site per second (times/s); t the contact time ($t = V/S_v$, s) and S_v is the flow rate of carrier gas (ml/s).

The activation energy (E_a) and the pre-exponential factor (A) can be obtained by plotting ln TOF versus $1/T$ according to the Arrhenius Eq. (4):

$$\ln TOF = \ln A - \frac{E_a}{RT} + \ln \left(\frac{VN_A}{22400V_b N_0} \right) \qquad (4)$$

where A is the pre-exponential factor; E_a the activation energy (J/mol); R the gas constant 8.314 (J/K); T the pulse temperature (K); V_b the preserve volume from the quantitative tube to the entrance of catalyst (ml) and $\ln(VN_A/(22400V_b N_0))$ is constant for every catalyst.

3. Results and discussion

3.1. Catalyst characterization

The XRD patterns of four Ni/α-Al$_2$O$_3$ catalysts with different Ni contents are show in Fig. 1. The peaks at 44.5° and 51.9° in the XRD patterns of the four catalysts can be, respectively, attributed
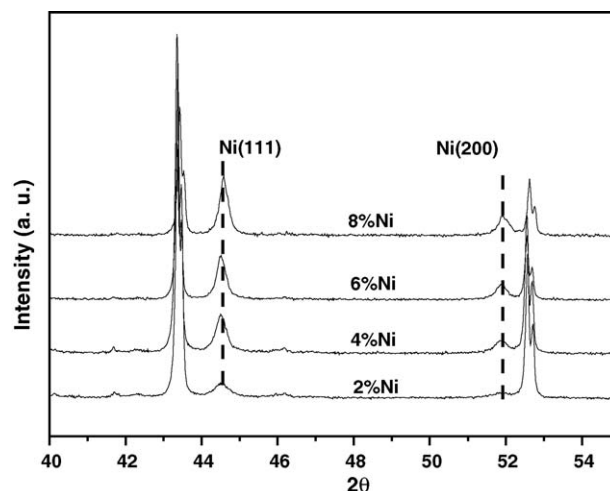

Fig. 1. The XRD patterns of the Ni/α-Al$_2$O$_3$ catalysts with different Ni content.

to Ni(1 1 1) and Ni(2 0 0) crystal planes. The only difference for the four samples is that the peaks intensity is increased with the Ni content. The unchanged location of peaks in the XRD patterns of Ni means the same lattice structure of Ni particles.

The average size of Ni crystal particles on Ni/α-Al$_2$O$_3$ can be calculated as 19.1, 31.8, 34.5 and 39.7 nm for the catalysts with the Ni content of 2, 4, 6 and 8% according to Scherrer formula, respectively (Table 1). The active sites of the four catalysts (the amount of exposed Ni atoms) are calculated according to the results of H$_2$-chemisorption (Table 1). The decrease in the average particle size increases the amount of the Ni active sites for per gram Ni. The dispersion degrees of Ni for the four catalysts are listed in Table 1, which are decreased with the increase in the Ni content of catalysts.

3.2. Preparation for the kinetic tests

The transfer of mass and heat should be firstly eliminated before the kinetic study for the CH_4 dissociation on the four Ni/α-Al$_2$O$_3$ catalysts. The reaction rates are exponentially increased with the reaction temperature; while the diffusion rates are linearly increased with the reaction temperature. Therefore, higher temperature makes the intrinsic kinetic rate increase faster than the diffusion rate. And the total rate is prone to be controlled by the diffusion at high reaction temperature. Therefore, the highest temperature used for the CH_4 pulse was chosen as the typical temperature to eliminate the diffusion.

The inner diffusion is eliminated by adjusting the sizes of catalyst grains (8%Ni as a model). The plot of the conversion of CH_4 versus the size of catalyst grain is shown in Fig. 2A. It was found that the conversions of CH_4 are increased with the decrease in the size of the catalyst grain. When the grain size of the catalyst is less than 0.175 nm (100–160 mesh), the conversions of CH_4 keep almost unchanged, meaning that the inner diffusion has been eliminated. The elimination of external diffusion can be performed by tuning the contact time of CH_4 gas and the catalyst to make the conversion of CH_4 linearly dependence on the contact time (shown as Fig. 2B). The contact time can
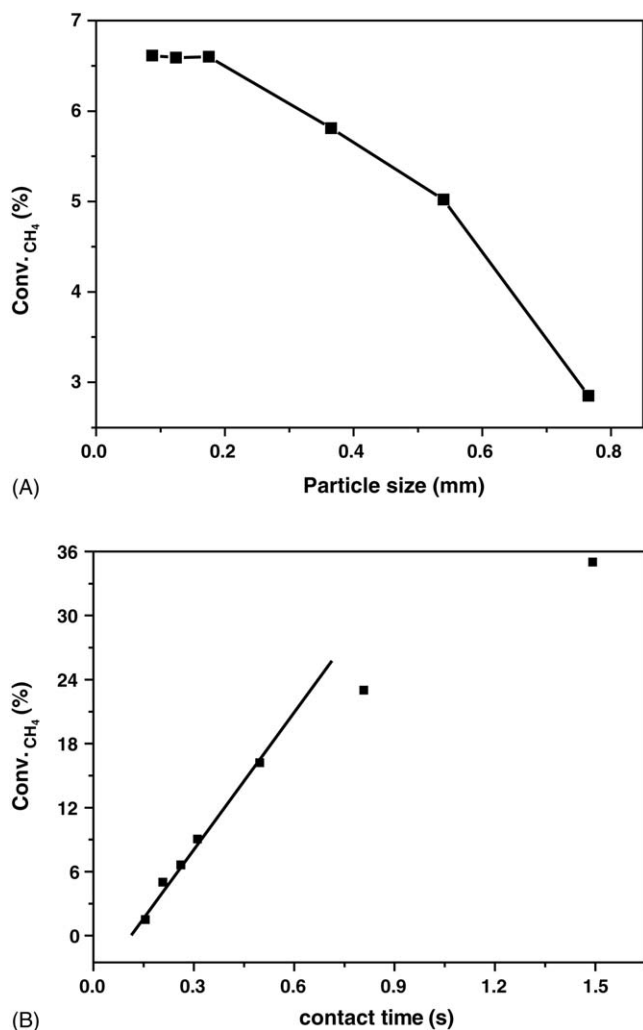
Fig. 2. The elimination of the inner diffusion (A) and the external diffusion (B) on 8%Ni/α-Al$_2$O$_3$ catalyst.

be tuned by changing the flow rate of carrier gas. It was found that the conversions of CH$_4$ become linear with the contact time when the contact time is less than 0.51 s. Meanwhile, the conversions of CH$_4$ are far away from the values of the thermodynamic equilibrium. The further increase in the contact time results in the departure of the conversion from the line. Therefore, the external diffusion can be eliminated with the contact time less than 0.51 s (Fig. 2B).

The conversion of CH$_4$ can be controlled by tuning the amount of catalyst and the flow rate of carrier gas in order to keep the temperature fluctuation of the catalyst bed within 0.5 K during the CH$_4$ pulse reaction. Then the heat transfer can be basically eliminated and the influence of the reaction heat on the catalytic reaction can be neglected.

3.3. Kinetic of CH$_4$ dissociation

The durative dissociation of CH$_4$ on the metal Ni sites generates the coke on the catalysts. Then the unsteady pulse experiments were carried out to avoid the deposition of carbon on Ni active sites, which greatly reduces the influence of carbon

species on the CH$_4$ dissociation. And the pulse reactions directly display the catalytic properties on the fresh Ni active sites of the Ni particles. The conversions of thermodynamic equilibrium at 748, 773, 798 and 823 K (Con$_{equ.}$%) are respectively calculated and listed in Table 2. The pulse conversions of CH$_4$ (Con$_{pul.}$%) on each catalyst at the different pulse temperature can be obtained by Eq. (1) and listed in Table 2. Notably, all the ratios of Con$_{pul.}$%/Con$_{equ.}$% at each temperature are lower than 20% and the pulse reactions are far away from the thermodynamic equilibrium.

The amount of the CH$_4$ dissociated on the Ni catalysts can be calculated based on the conversions of the CH$_4$ pulse (Con$_{pul.}$%). And the coverage degree of carbon species on the Ni active sites (C$_{coverage}$%) can be calculated according to Eq. (2) and listed in Table 2. The values of C$_{coverage}$% at different temperature are all less than 1, meaning that the dissociation of CH$_4$ is mainly carried out on the fresh Ni active sites and the influence of the carbon deposition on the CH$_4$ dissociation can be neglected. Therefore, the pulse reactions give the intrinsic kinetic information of the CH$_4$ dissociation on the fresh Ni active sites of the Ni particles.

The TOF$_{CH_4}$ for the pulse reaction on per Ni active site at different reaction temperature can be calculated according to Eq. (3) and listed in Table 2. The TOF$_{CH_4}$ was found to increase with the increase in the pulse temperature for every catalyst. And it should be noted that the TOF$_{CH_4}$ obtained for the Ni/α-Al$_2$O$_3$ with different loading amount of Ni is not the same at the same pulse temperature. The different loading of Ni on Ni/α-Al$_2$O$_3$ results in the different Ni particle sizes. Therefore, the TOF$_{CH_4}$ should be related with the Ni nano particles with different sizes. The relationship between the TOF$_{CH_4}$ and particle sizes of Ni on four catalysts at every pulse temperature is shown in Fig. 3. The increase in the nano-scale of Ni particles from 19.1 to 31.8 nm increases the TOF$_{CH_4}$, and the further increasing the particle sizes decreases the TOF$_{CH_4}$. The highest TOF$_{CH_4}$ was obtained for the catalyst with Ni particle size of 31.8 nm at each pulse temperature. The plots of TOF$_{CH_4}$ versus particle size of Ni at each temperature show "mountain" shapes in Fig. 3. It has
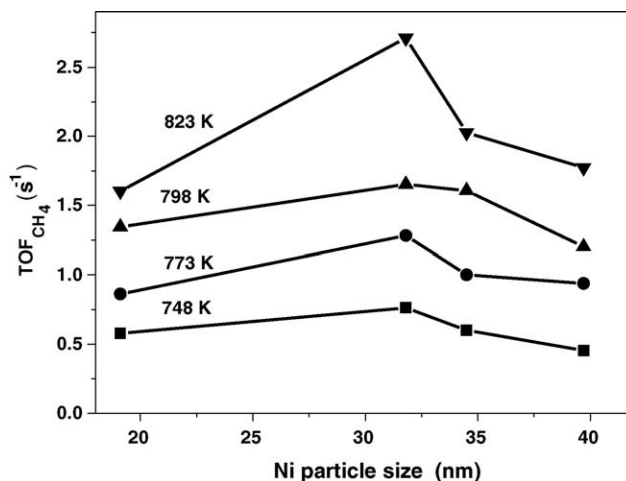

Fig. 3. The effect of Ni nano-scale particles on the TOF at different pulse temperature.

Table 3
E_a and A of CH_4 dissociation on the Ni/α-Al$_2$O$_3$ catalysts with different Ni content

Catalyst	E_a (kJ/mol)	A (10^7)
2%Ni	73.2	0.18
4%Ni	83.5	1.50
6%Ni	86.1	2.25
8%Ni	90.9	6.12

Calculated based on Fig. 4 according to Eq. (4).

Fig. 5. The relationship of the E_a for the dissociation of CH_4 vs. the Ni particle sizes on the four catalysts.

been reported that one reaction can be defined as a structure sensitive reaction when the reaction activity (TOF) is changed with the metal particle size [18,19]. For example [20], the CO hydrogenation reaction on Rh catalyst is a structure sensitive reaction because the TOF for the hydrogenation of CO is varied with the particle sizes of Rh on Rh/γ-Al$_2$O$_3$ catalysts. Recently, Lu et al. [21] found that ethylene epoxidation on Ag catalyst is a structure sensitive reaction since the bigger Ag particles produce higher epoxidation activity. The "mountain" shapes of TOF$_{CH_4}$ versus the Ni particle size provide the direct evidence for the structure sensitive reaction of CH_4 dissociation on Ni catalyst.

The pulse reaction is performed in the kinetic region and the E_a and A further elucidate the influence of the Ni particle sizes on the TOF$_{CH_4}$ of CH_4 dissociation. The plots of lnTOF$_{CH_4}$ versus $1/T$ according to Eq. (4) for every catalyst are shown in Fig. 4. These plots show good linear relationship for every catalyst. Then E_a and A for the CH_4 dissociation on every catalyst can be calculated based on Fig. 4 according to Arrhenius formula and listed in Table 3. The E_a for CH_4 dissociation on the four catalyst is 2%Ni (73.2 kJ/mol) < 4%Ni (83.5 kJ/mol) < 6%Ni (86.1 kJ/mol) < 8%Ni (90.9 kJ/mol). The pre-exponential fac-
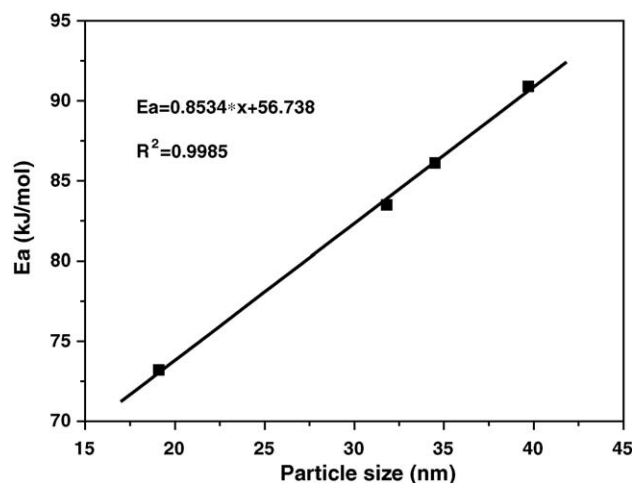
tor A for CH_4 dissociation on each catalyst is: 2%Ni (0.18 × 10^7) < 4%Ni (1.50 × 10^7) < 6%Ni (2.25 × 10^7) < 8%Ni (6.12 × 10^7). Both the E_a and A of CH_4 dissociation are increased with the increase in the Ni particle size. Then plot of E_a versus the Ni nano-scale particles shows a good linear relationship with the correlated coefficient R^2 of 0.9985 (Fig. 5). And ln$A$ is also well linear versus the Ni particle size with the correlated coefficient R^2 of 0.9988 (Fig. 6). The increase in the sizes of Ni nano particles linearly increases the E_a and ln$A$, which further confirms that the CH_4 dissociation reaction on Ni/α-Al$_2$O$_3$ catalyst is a structure sensitive reaction from the viewpoint of the kinetics.
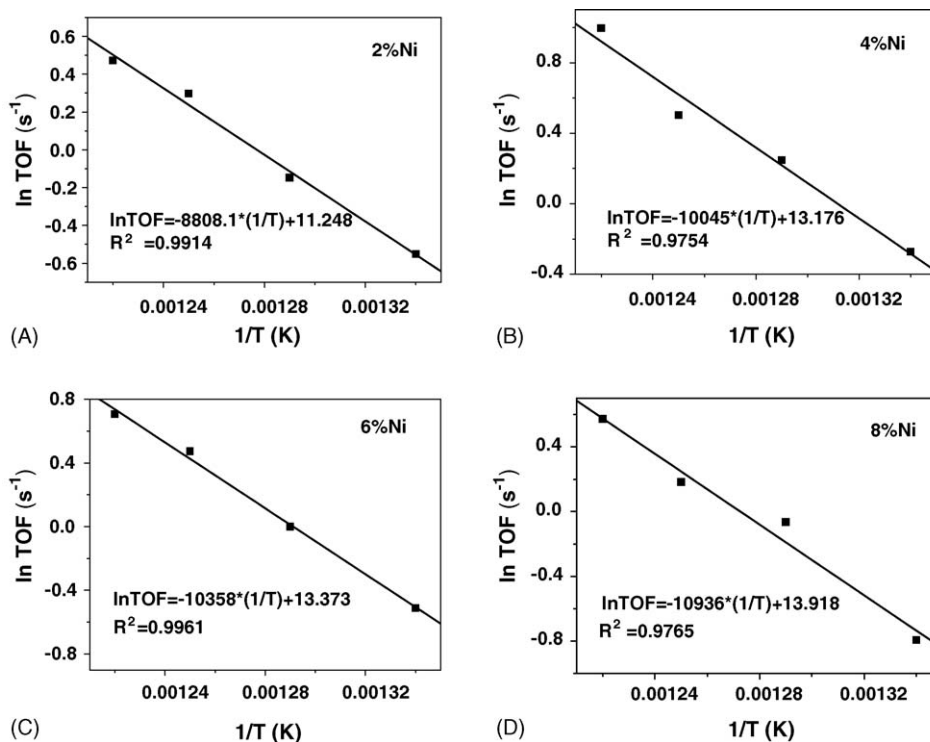

Fig. 4. The relationship of ln TOF vs. $1/T$ for the CH_4 pulse dissociation on the four catalysts.
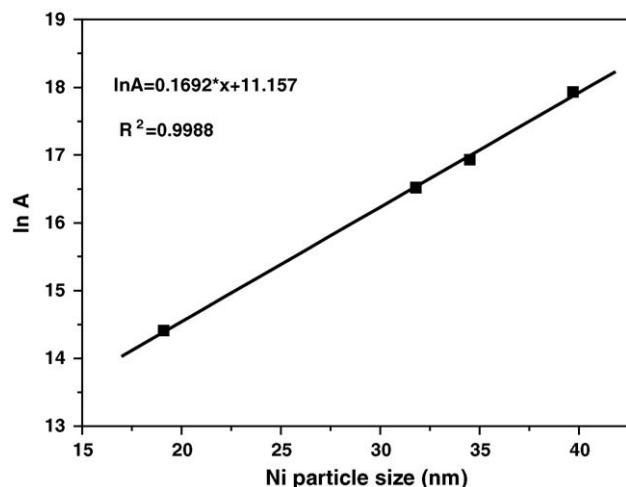
Fig. 6. The relationship of the $\ln A$ for the dissociation of CH_4 vs. the Ni particle sizes on the four catalysts.

It has been reported [22] that the nickel particles with difference size have the different type of lattice planes exposed. Both the theory calculation and experiment results [7–9] show that the dissociation of CH_4 on the different crystal plans of Ni metal gives the different activation energy. Burghgraef et al. [23] calculated based on the electron structure of Ni that the activation energy of CH_4 dissociation is increased with the increase in the atoms number of Ni particle: that the E_a of CH_4 dissociation on one Ni atom is $40.7 \, \text{kJ mol}^{-1}$ and the E_a on Ni_{13} particle is increase to $99.7 \, \text{kJ mol}^{-1}$. These results may be used to explain that the E_a for the CH_4 dissociation was changed with the different Ni particle size.

The general equation for the compensation effect [24,25] is shown below:

$$A = A_0 \exp(cE_a) \quad \text{or} \quad \ln A = cE_a + \ln A_0 \tag{5}$$

where A_0 and c are two constants.

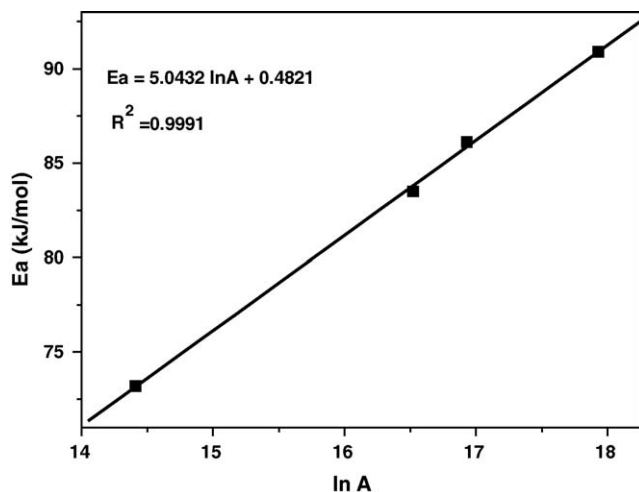The plot of $\ln A$ versus E_a obtained from the CH_4 dissociation on the different Ni particles is shown in Fig. 7. It is worth noted that the $\ln A$ is well linear with the E_a for the CH_4 pulse dissociation reaction and the correlation coefficient R^2 is up to 0.9991. E_a and $\ln A$ are linearly increased with the increase in the Ni particle size. The compensation effect is proved to be present in the CH_4 pulse dissociation on $Ni/\alpha\text{-Al}_2O_3$ catalyst, which further indicates that the kinetic parameters obtained here are correlated with the intrinsic kinetic properties of the fresh Ni active sites. The compensation effect of E_a and A results in the "mountain" shape of the plots of TOF_{CH_4} versus Ni particle sizes in Fig. 3. This work proves that the CH_4 dissociation on $Ni/\alpha\text{-Al}_2O_3$ is a structure sensitive reaction based on the linear relationship of E_a and $\ln A$ with Ni particle size.

4. Conclusions

In conclusion, the pulse of CH_4 through $Ni/\alpha\text{-Al}_2O_3$ with different Ni particle sizes gives the intrinsic kinetic information of the single dissociation of CH_4 on the fresh Ni active sites of the Ni particles. The plots of the TOF_{CH_4} versus Ni particle size show a "mountain" shape at each pulse temperature. The dissociation of CH_4 on Ni catalyst is proved to be a structure sensitive reaction. E_a and $\ln A$ obtained from the intrinsic kinetic of the CH_4 dissociation were found to linearly increase with the Ni particle size. The $\ln A$ is well linear with the E_a for the CH_4 pulse reaction and the compensation effect of E_a and A is present in the CH_4 dissociation on $Ni/\alpha\text{-Al}_2O_3$. This work proves that the CH_4 dissociation on $Ni/\alpha\text{-Al}_2O_3$ is a structure sensitive reaction based on the linear relationship of E_a and $\ln A$ with Ni particle size.

References

[1] M.C.J. Bradford, M.A. Vannice, Catal. Rev. Sci. Eng. 41 (1999) 1.
[2] K. Otsuka, S. Takenaka, H. Ohtsuki, Appl. Catal. A 273 (2004) 113.
[3] K. Otsuka, T. Seino, S. Kobayashi, S. Takenaka, Chem. Lett. (1999) 1179.
[4] Q. Liang, L.Z. Gao, Q. Li, S.H. Tang, B.C. Liu, Z.L. Yu, Carbon 39 (2001) 897.
[5] J. Jai, Y. Wang, E. Tanabe, T. Shishido, K. Takehira, Microporous Mesoporous Mater. 57 (2003) 283.
[6] M.-S. Liao, Q.-E. Zhang, J. Mol. Catal. A. 136 (1998) 185.
[7] A.P.J. Jansen, H. Burghgraef, Surf. Sci. 344 (1995) 149.
[8] H.S. Beengaard, I. Alstrup, I. Chorkendorff, S. Ullmann, J.R. Rostrup-Nielsen, J.K. Norskov, J. Catal. 187 (1999) 238.
[9] H. Yang, J.L. Whitten, Surf. Sci. 289 (1993) 30.
[10] T.P. Beebe Jr., D.W. Goodman, B.D. Kay, J. Chem. Phys. 87 (1987) 2305.
[11] R.C. Egeberg, S. Ullmann, I. Alstrup, C.B. Mullins, I. Chorkendorff, Surf. Sci. 497 (2002) 183.
[12] M.A. Ermakova, D.Y. Ermakov, G.G. Kuvshinov, Appl. Catal. A 201 (2000) 61.
[13] G.G. Kuvshinov, Y.I. Mogilnykh, D.G. Kuvshiov, Catal. Today 42 (1998) 357.
[14] I. Alstrup, M.T. Tavares, J. Catal. 139 (1993) 513.

Fig. 7. The relationship between the E_a and A for the CH_4 dissociation on the four catalysts.

[15] S. Takenaka, E. Kato, Y. Tomikubo, K. Otsuka, J. Catal. 219 (2003) 176.
[16] S. Takenaka, S. Kobayshi, H. Ogihara, K. Otsuka, J. Catal. 217 (2003) 79.
[17] T. Borowiecki, G. Giecko, M. Panczyk, Appl. Catal. A 230 (2002) 85.
[18] M. Boudart, J. Mol. Catal. 30 (1985) 27.
[19] J.J. Carberry, J. Catal. 114 (1988) 277.
[20] M. Ojeda, S. Rojas, M. Boutonnet, F.J. Pérez-Alonso, F.J. García-García, J.L.G. Fierro, Appl. Catal. A 274 (2004) 33.
[21] J. Lu, J.J. Bravo-Suarez, A. Takahashi, M. Haruta, S.T. Oyama, J. Catal. 232 (2005) 85.
[22] M.L. Toebes, J.H. Bitter, A.J.V. Dillen, K.P.D. Jong, Catal. Today 76 (2002) 33.
[23] H. Burghgraef, A.P.J. Jansen, R.A.V. Santen, Faraday Discuss. 96 (1993) 337.
[24] G. Scheab, Adv. Catal. 2 (1950) 251.
[25] W.M.C. Conner Jr., J. Catal. 78 (1982) 238.